# A reliability-operational analysis of a track-side CCTV cabinet taking into account interference

Jacek PAŚ [1], Adam ROSIŃSKI [2]*, and Kamil BIAŁEK [3]

[1] Military University of Technology, ul. gen. S. Kaliskiego 2, 00-908 Warsaw, Poland
[2] Warsaw University of Technology, ul. Koszykowa 75, 00-662 Warsaw, Poland
[3] Railway Institute, ul. Chłopickiego 50, 04-275 Warsaw, Poland

**Abstract.** The paper presents issues associated with the impact of electromagnetic interference on track-side cabinets of a closed-circuit television system (CCTV) functioning in a railway transport environment. The measurements of an electromagnetic field emitted by a track-side CCTV cabinet were presented. Designs of this kind are operated in railway facilities; therefore, they should not disturb the functioning of other equipment, the rail traffic control systems, in particular (the so-called inner compatibility). An analysis of the obtained results facilitated developing a research model, and, further, improving its reliability and conducting an operational analysis, considering electromagnetic interference. This enabled us to determine a relationship allowing us to specify the probability of a track-side CCTV cabinet staying in a state of full ability. The presented discussions regarding a track-side CCTV cabinet, considering electromagnetic interference, allow us for the numerical assessment of different types of solutions (technical and organizational), which can be implemented in order to mitigate the impact of electromagnetic interference on the system functioning.

**Key words:** operation; reliability; electromagnetic interference; modelling; closed-circuit television.

## 1. Introduction

CCTV systems are used in various branches of transport (critical infrastructure) in order to ensure the travellers' safety [1,2]. They are also used in railway transport [3–6], most often functioning in diverse operating conditions. The observations of their operating process in a railway environment confirm the dependency of their correct operation on the reliability of the system components, and an efficient operational management process [7–9]. Therefore, a thorough analysis of the reliability-operating phenomena of CCTV systems should consider not only their reliability, but also the efficiency of operational management [10]. For this purpose, the authors imitated the phenomena occurring in reality (including electromagnetic interference) in a research model of a track-side CCTV cabinet.

CCTV systems are currently very often used in transport systems (critical infrastructure). Their correct operation significantly impacts the safety and efficiency of a transport process [11, 12]. The unreliability of these devices in terms of safety may lead to traffic safety hazards [13]. The theory of reliability deals with the analysis of the damaging impact on specified reliability indicators [14, 15], among others. The area of interest of the safety theory includes the results of damage, which lead to safety hazards (especially, from the point of view of a transport process, as well as traffic control) [16, 17]. Therefore, the issue of correctly defining which state of the system can be deemed permissible or unacceptable from the point of view of safety (impendency over safety states) is very important.

Increasing the safety level of transport systems can be achieved by improving their reliability parameters, among others. The reliability of a track-side CCTV cabinet is impacted by both the reliability of its components, as well as the use of redundant structures. The first solution is aimed at preventing damage. In the second case, the use of redundancy, although leading to an expansion of the system, enables tolerating the occurring damage (through the introduction of impendency over safety states) [18]. Redundancy can apply to both sub-assemblies of the device, as well as external power supply systems or data transmission paths [19]. The quality of information [20–22] obtained by the systems from the sensors or cameras [23–26] is also important during a reliability-operational analysis. Some authors suggest the use of artificial neural networks [27, 28] or fuzzy logic [29] in their research papers. The functioning of a track-side CCTV cabinet is also significantly impacted by the vibrations generated as a result of rail vehicle movement [30, 31] but they are not considered in this article.

Assessing the impact of electromagnetic interference on the operation of transport systems has been the subject of scientific research for a long time [32, 33]. The analyses concern not only mobile means of transport but also stationary facilities. However, we still lack detailed elaborations containing both the deliberations in the field of electromagnetic compatibility measurements, as well as the reliability-operational analysis.

The evaluation of electromagnetic compatibility considering the impact of atmospheric discharges on the operation of various electronic devices has been so far discussed in regard to railway transport, among others. The electronic devices used

in transport include i.e. rail traffic control systems, systems installed at level crossings, GSM-R (Global System for Mobile Communications – Railway), visual monitoring systems, etc. The analyses in that field were presented in paper [34]. The authors previously presented various methods of protection against adverse phenomena of such type. They also described solutions increasing the protection efficiency (i.e. through the arrangement of electronic devices adequate to the environmental conditions already at the engineering stage of the systems and protective elements).

Paper [35] should be cited among the scientific works in the field of ensuring electromagnetic compatibility of electronic systems and devices. The elaboration describes important issues associated with using various materials for the construction of mobile means of transport and their impact on satisfying the requirements of electromagnetic compatibility (including screening).

Another group of publications includes deliberations in the field of electromagnetic interference and electromagnetic compatibility of electronic safety systems [36, 37], including CCTVs in particular. The authors of these papers present a generic approach towards this issue, not considering the specific nature of rail transport and the requirements therein.

The publication [38, 39] presents issues regarding electromagnetic interference emitted by CCTV systems. Their authors paid particular attention to the electromagnetic radiation emission by individual devices constituting the studied CCTV system. It was generally concluded that the limit values were exceeded. Hence, a tested system can adversely impact the functioning of other electronic devices nearby. Therefore, it is necessary to search for solutions mitigating the impact of electromagnetic interference on other devices.

The issue of decreasing electromagnetic interference emissions in CCTV systems was discussed in [40]. The study included all kinds of leaks in the metal housings of the cabinets, as well as a power cable and transmission bus penetrations, which can appear within the screening of various equipment. It was concluded that such structural solutions have a high impact on the possibility of exceeding permissible emission levels and meeting EMC requirements.

A similar approach, as in the aforementioned article, was presented in the publications [41]. The authors studied the impact of electromagnetic interference on the functioning of electronic devices (forming an intrusion detection system). It was concluded that at high frequencies (i.e. 988 MHz), the system will erroneously signal a state of alarm.

The previous considerations (presented above) in the field of electromagnetic compatibility of CCTV systems, considering electromagnetic interference, and the suggestions of solutions decreasing the level of electromagnetic interference, do not take reliability-operational modelling into account. This is why the authors of this article decided to adopt such an approach while bearing in mind the specificity of rail transport and the applicable normative requirements [42–45].

The paper presents the measurements of an electromagnetic field emitted by a track-side CCTV cabinet. Technical solutions of this kind are installed in railway objects; therefore, they should not disturb the functioning of other equipment, the rail traffic control systems, in particular. An analysis of the obtained results enabled us to develop a research model, and a further reliability-operational analysis, considering electromagnetic interference.

## 2. Reliability-operational analysis of a track-side CCTV cabinet with regard to electromagnetic interference

The radiated interference emissions of a track-side CCTV cabinet on level crossing were measured in "in situ" conditions, at a distance of 3 m, over a frequency band of 30 MHz to 1 GHz. Two types of antennas, which enable complete coverage (measurement) of the specific frequency range were used for measuring the radiated interference emissions over the frequency band of 30 MHz to 1 GHz.

The following antenna types were used to measure the radiation interference emissions:

- A biconical antenna enabling the measurement of an electric field component, over a frequency range from 30 MHz to 230 MHz. The measurement is taken for vertical and horizontal polarization of an electromagnetic wave – Fig. 1.
- A log-periodic antenna enabling the measurement of an electric field component, over a frequency range from 230 MHz to 1 GHz. The measurement is taken for vertical and horizontal polarization of an electromagnetic wave – Fig. 2.
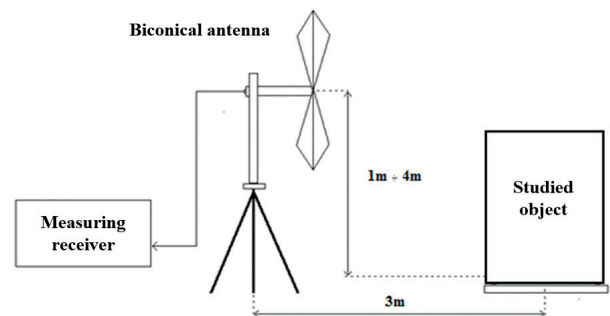


Fig. 1. Diagram of a stand for measuring the electric field intensity over a frequency range from 30 MHz to 230 MHz
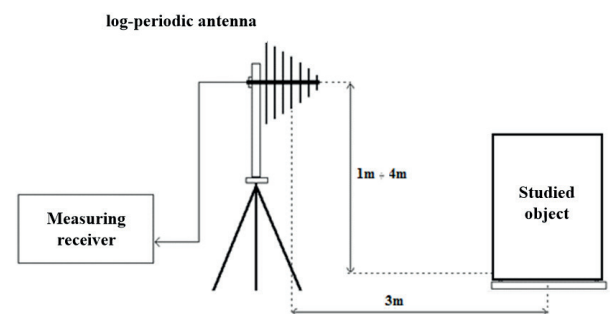


Fig. 2. Diagram of a stand for measuring the electric field intensity over a frequency range from 230 MHz to 1 GHz

2

Bull. Pol. Acad. Sci. Tech. Sci. 69(2) 2021, e136747

The source of electromagnetic interference should be at a certain distance from the measurement system, in this case, the measurement antenna, the type of which depends on the frequency range of the interfering signals. To measure the component of the electric field strength E we use two different types of antennas, depending on the range of measured frequencies – Fig. 1 biconical antenna frequency range from 30 MHz to 230 MHz, while for the frequency range 230 MHz, it is 1 GHz – Fig. 2 log-periodic antenna. The height of the antenna (1–4 m) during the measurement is determined by the influence of the ground plane and objects, e.g. metal, that may be in a considered area and influence the distortion of the electromagnetic field by the so-called secondary radiation. The measurement distance of 3 m is determined by the frequency range of the interfering signals.

The electromagnetic field background measurement was conducted for a frequency range from 30 MHz to 1 GHz. The green colour on the graphs marks the course of the electromagnetic field background measurement for the individual frequency sub-ranges. The red colour marks a measurement with an activated track-side CCTV cabinet. The measurement was conducted over a vast railway area, excluding the impact of non-stationary interference generated by interference sources, which are found in an electric train unit. The exceeded limit values of the electromagnetic field over a frequency band of 30 MHz–50 MHz, with its source being a track-side CCTV cabinet, were observed during the radiated interference emission measurements.

The measurements were conducted with the use of an EMI ESCI3 measurement receiver and two antennas:
- a VBA 6106A biconical antenna,
- a VUSLP 9111B log-periodic antenna.

The used measuring equipment satisfied the requirements of the standard [46]. The measurements were conducted as per the methodology presented in the standard [47]. Electromagnetic radiation limit values were adopted as per the guidelines included in the standard for railway objects [48, 49].

Electromagnetic compatibility (EMC) test involved a track-side CCTV cabinet consisting of:
- a rectifier power plant,
- an AC/DC converter,
- an IP amplifier,
- a modem,
- a screen,
- an IP server,
- a recorder.

The cabinet is supplied by AC power from a 230V AC industrial power grid.

The radiated interference emission measurement for a frequency band of 30 MHz ÷ 230 MHz and vertical antenna polarization is shown in Fig. 3. Table 1 shows the values of frequencies at which the radiated interference emission limits were exceeded over the frequency range of 30 MHz ÷ 230 MHz for vertical antenna polarization. The radiated interference emission measurement for a frequency band of 30 MHz ÷ 230 MHz and horizontal antenna polarization is shown in Fig. 4. Table 2

shows the values of frequencies at which the radiated interference emission limits were exceeded over the frequency range of 30 MHz ÷ 230 MHz for horizontal antenna polarization.
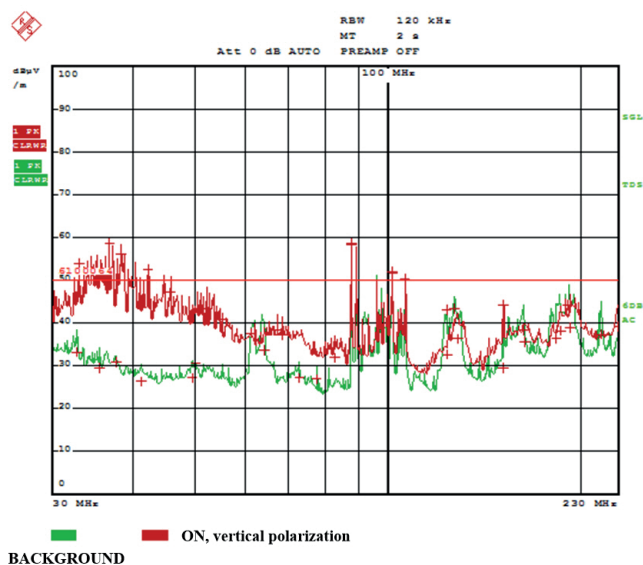


Fig. 3. The radiated interference emission measurement for a frequency range of 30 MHz–230 MHz and vertical antenna polarization
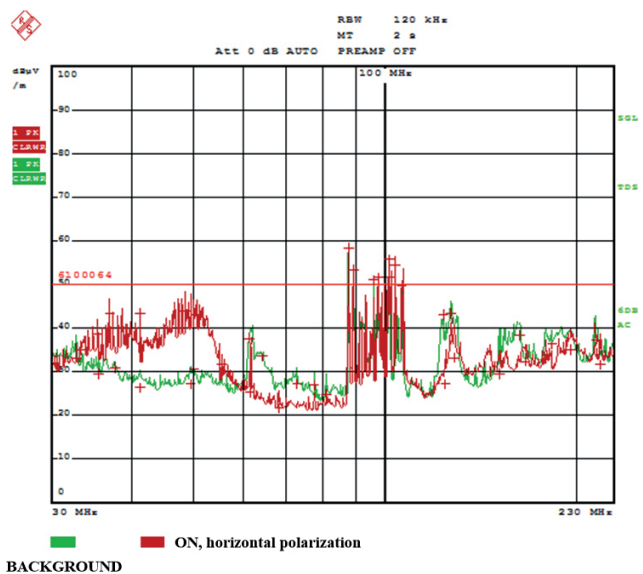


Fig. 4. Radiated interference emission measurement for a frequency range of 30 MHz–230 MHz and horizontal antenna polarization

Radiated interference emission measurement for a frequency band of 230 MHz–1 GHz and vertical antenna polarization is shown in Fig. 5. Table 3 shows the values of frequencies at which the radiated interference emission limits were exceeded over the frequency range of 230 MHz–1 GHz for the vertical antenna polarization. The radiated interference emission measurement for a frequency band of 230 MHz–1 GHz and horizontal antenna polarization are shown in Fig. 6. Table 4 shows the values of frequencies at which the radiated interference

Bull. Pol. Acad. Sci. Tech. Sci. 69(2) 2021, e136747

3

J. Paś, A. Rosiński, and K. Białek

Table 1

The values of frequencies at which the radiated interference emission limits were exceeded over the frequency range of 30 MHz–230 MHz for vertical antenna polarization

| Frequency value [MHz] | Value of the amplitude of disturbing signal U [dBμV] for radiated interference emission levels over a frequency level of 30 MHz–230 MHz – background level | Frequency value [MHz] | Value of the amplitude of disturbing signal U [dBμV] for radiated interference emission levels over a frequency level of 30 MHz–230 MHz – device on |
|---|---|---|---|
| 87 | 58 | 32–42 (frequency band) | max 58 |
| 101 | 52 | 87 | 59 |
| – | – | 89 | 57 |
| – | – | 101 | 52 |
| – | – | 106 | 51 |

Table 2

The values of frequencies at which the radiated interference emission limits were exceeded over the frequency range of 30 MHz–230 MHz for horizontal antenna polarization

| Frequency value [MHz] | Value of the amplitude of disturbing signal U [dBμV] for radiated interference emission levels over a frequency level of 30 MHz–230 MHz – background level | Frequency value [MHz] | Value of the amplitude of disturbing signal U [dBμV] for radiated interference emission levels over a frequency level of 30 MHz–230 MHz – device on |
|---|---|---|---|
| 88 | 58 | 88 | 58 |
| 89 | 54 | 89 | 54 |
| 95 | 51 | 96 | 52 |
| 101 | 55 | 101 | 55 |
| 104 | 55 | 104 | 55 |
| – | – | 106 | 53 |

emission limits were exceeded over the frequency range of 230 MHz–1 GHz for the horizontal antenna polarization.

The result was a conclusion that for some frequency ranges, the limit values were exceeded. Therefore, there is a need for further research in order to develop efficient methods for mitigating electromagnetic interference.

Very low-frequency disturbing signals, e.g. from the power grid, do not affect the operation of electronic safety systems.
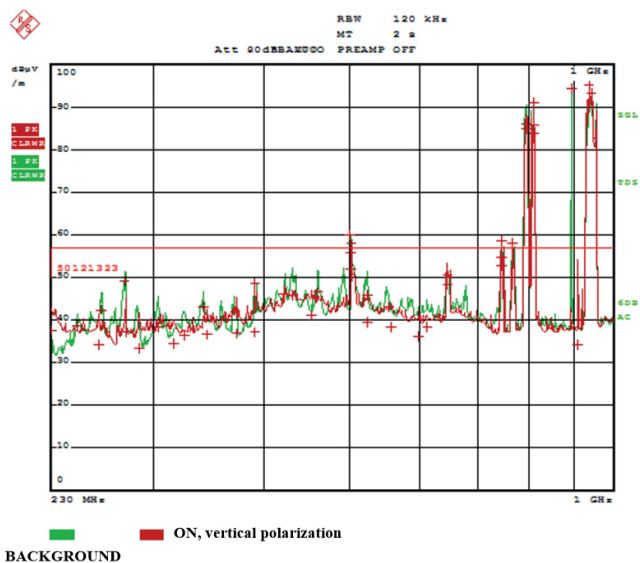


Fig. 5. Radiated interference emission measurement for a frequency range of 230 MHz–1 GHz and vertical antenna polarization
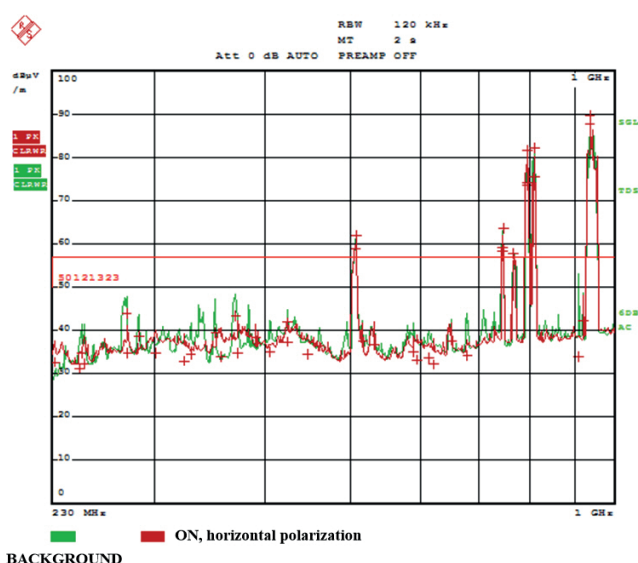


Fig. 6. Radiated interference emission measurement for a frequency range of 230 MHz–1 GHz and horizontal antenna polarization

4

Bull. Pol. Acad. Sci. Tech. Sci. 69(2) 2021, e136747

Table 3
The values of frequencies at which the radiated interference emission limits were exceeded over the frequency range of 230 MHz–1 GHz for vertical antenna polarization

| Frequency value [MHz] | Value of the amplitude of disturbing signal U [dBμV] for radiated interference emission levels over a frequency level of 230 MHz–1 GHz – background level | Frequency value [MHz] | Value of the amplitude of disturbing signal U [dBμV] for radiated interference emission levels over a frequency level of 230 MHz–1 GHz – device on |
|---|---|---|---|
| 500 | 60 | 500 | 60 |
| 750 | 59 | 750 | 59 |
| 780 | 58 | 780 | 58 |
| 780–810 (frequency range) | max 90 | 780–810 (frequency range) | max 91 |
| 897 | 95 | 940–970 (frequency range) | max 95 |
| 940–970 (frequency range) | max 96 | – | – |

Table 4
The values of frequencies at which the radiated interference emission limits were exceeded over the frequency range of 230 MHz–1 GHz for horizontal antenna polarization

| Frequency value [MHz] | Value of the amplitude of disturbing signal U [dBμV] for radiated interference emission levels over a frequency level of 230 MHz–1 GHz – background level | Frequency value [MHz] | Value of the amplitude of disturbing signal U [dBμV] for radiated interference emission levels over a frequency level of 230 MHz–1 GHz – device on |
|---|---|---|---|
| 508 | 61 | 508 | 62 |
| 750 | 63 | 750 | 58 |
| 780 | 58 | 780 | 58 |
| 780–810 (frequency range) | max 82 | 780–810 (frequency range) | max 82 |
| 940–970 (frequency range) | max 90 | 940–970 (frequency range) | max 90 |

In this frequency range, there are distinguished two measuring ranges for interference signals: ELF (extremely low frequencies 5 Hz to 2 kHz) and VLF (very low frequencies 2 kHz to 100 kHz). The value of disturbing signals in a given space, where the elements of electronic safety systems are used, do not exceed the acceptable level of safety for the use process. The sources of interference in this frequency range generate components of the electromagnetic field E, H that do not affect the use process.

In the course of analyzing the measurement results, it can be concluded that a track-side CCTV cabinet operated in a railway transport environment (with electromagnetic interference present [50, 51]) can stay in defined states [52–54]. Therefore, it was decided to conduct a reliability-operational analysis [55, 56]. This will enable the determination of the relationships that allow us to calculate the values of the probabilities of the track-side CCTV cabinet staying in the distinguished states of operation.

An example of a video monitoring system diagram is shown in Fig. 7.

The mechanism of electromagnetic interference penetrating railway device circuits is called coupling. A track-side CCTV
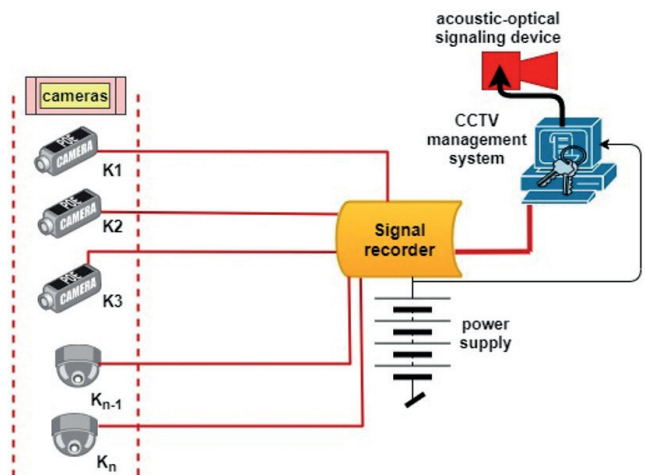


Fig. 7. The structure of a typical CCTV

Bull. Pol. Acad. Sci. Tech. Sci. 69(2) 2021, e136747

5

cabinet, as shown in Fig. 8, is subject to the impact of the radiated electromagnetic field (EMF) interference over a broad range of frequencies. A transmission bus or a power cable of a track-side CCTV cabinet "collects" the HF disturbing current with this cable. This phenomenon appears as a result of EMF coupled with this cable. A track-side CCTV cabinet power cable/transmission bus shall be treated as a receiving antenna in this case. The interference current induced in the a/m cables under the influence of EMF, together with the useful signal, is supplied to a track-side CCTV cabinet. The useful signal, together with the disturbing current, disturbs the track-side CCTV cabinet reference potential as a result of coupling through common impedance Z. Serial (through EMF) and parallel (Z and C) coupling is executed in a track-side CCTV cabinet. The coupling is executed by the following elements: reference Z and capacitance C impedance of a PCB board relative to a metal casing of the cabinet. Coupling of the board with the metal casing may be mitigated by decreasing the parasitic capacitance between a circuit particularly sensitive to the interference present in a given device and the ground, or by decreasing the fast transient voltage present at this capacitance. The interference voltage present on common reference impedance Z may result in the appearance of coupling through crosstalk – inductive or capacitive in electrical cables, which are located near an interference source – $U_{zak}$. The difference in the potential between the cable and the track-side CCTV cabinet environment creates an electric field around this cable. A variable electric field, in turn, generates a current which is induced in the cables located near a transmission bus (the so-called capacitive crosstalk – $C_{pp}$). The coupling is proportional to the rate of the interference voltage changes over time.
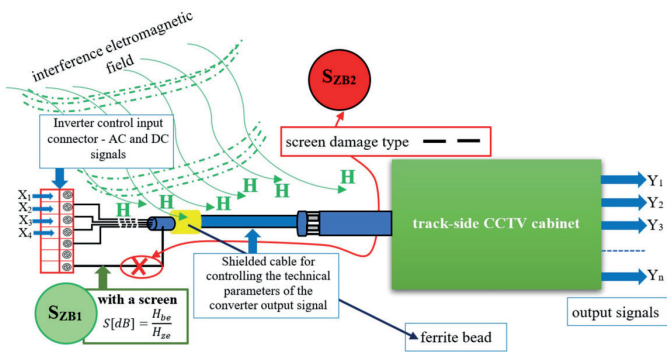


Fig. 8. Impact of interference on a track-side CCTV cabinet

Designations in the fig.:
S [dB] – screening efficiency
$H_{be}$ – the strength of the component of the magnetic field without the shield
$H_{ze}$ – the intensity of the component of the magnetic field with the shield
$S_{ZB1}$ – the state of impendency over safety I
$S_{ZB2}$ – the state of impendency over safety II
H – the magnetic component of the electromagnetic field
$Y_1, Y_1, \ldots, Y_n$ – output signals
$X_1, X_2, X_3, X_4$ – input signals

In the course of conducting an operational analysis regarding a track-side CCTV cabinet, it is possible to illustrate the relationships occurring in such a structure, in terms of reliability and operation, as presented in Fig. 9.
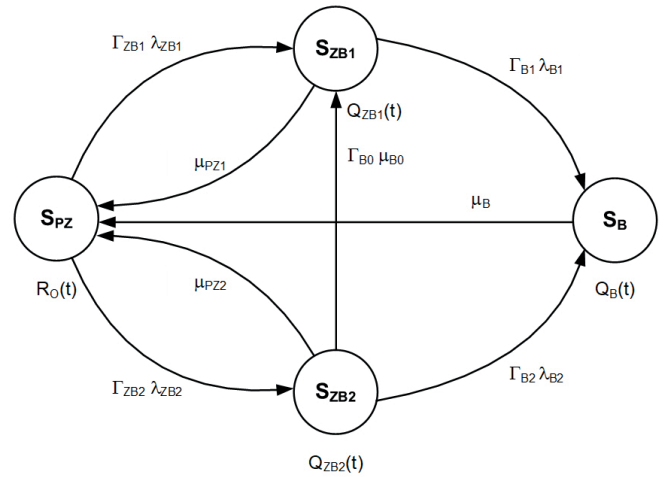


Fig. 9. Relations in a track-side CCTV cabinet, taking into account electromagnetic interference

Designations in the figure:
$R_O(t)$ – probability function of the system staying in the state of full ability $S_{PZ}$
$Q_{ZB1}(t)$ – the probability function of a system staying in a state of impendency over safety I $S_{ZB1}$
$Q_{ZB2}(t)$ – the probability function of a system staying in a state of impendency over safety II $S_{ZB2}$,
$Q_B(t)$ – the probability function of a system staying in a state of the unreliability of safety $S_B$
$\lambda_{ZB1}$ – intensities of transition from a state of full ability $S_{PZ}$ to a state of impendency over safety I $S_{ZB1}$
$\lambda_{ZB2}$ – intensities of transition from a state of full ability $S_{PZ}$ to a state of impendency over safety II $S_{ZB2}$
$\mu_{PZ1}$ – intensities of transition from a state of impendency over safety I $S_{ZB1}$ to a state of full ability $S_{PZ}$
$\mu_{PZ2}$ – intensities of transition from a state of impendency over safety II $S_{ZB2}$ to a state of full ability $S_{PZ}$
$\mu_{B0}$ – intensities of transition from a state of impendency over safety II $S_{ZB2}$ to a state of full ability I $S_{PZ}$
$\mu_{B1}$ – intensities of transition from a state of the unreliability of safety $S_B$ to a state of full ability $S_{PZ}$
$\lambda_{B1}$ – intensities of transition from a state of impendency over safety I $S_{ZB1}$ to a state of the unreliability of safety $S_B$
$\lambda_{B2}$ – intensities of transition from a state of impendency over safety II $S_{ZB2}$ to a state of the unreliability of safety $S_B$
$\Gamma_{ZB1}$ – the electromagnetic interference factor for the transition intensity $\lambda_{ZB1}$
$\Gamma_{ZB2}$ – the electromagnetic interference factor for the transition intensity $\lambda_{ZB2}$
$\Gamma_{B1}$ – the electromagnetic interference factor for the transition intensity $\lambda_{B1}$
$\Gamma_{B2}$ – the electromagnetic interference factor for the transition intensity $\lambda_{B2}$
$\Gamma_{B0}$ – the electromagnetic interference factor for the transition intensity $\mu_{B0}$

6

Bull. Pol. Acad. Sci. Tech. Sci. 69(2) 2021, e136747

In order to reduce the influence of electromagnetic interference on the functioning of the track-side CCTV cabinets, various solutions are used (e.g. screening, the filtration of power and signal lines, the separation of cable routes, the use of optical fibres). In the developed model it was assumed that it would be determined by the factor of electromagnetic interference $\Gamma$. It will be characteristic for each of the intensities of transitions between the distinguished states. It was assumed that it will have the following value:

$$\Gamma \in \langle 0,1 \rangle . \tag{1}$$

We assume that:
- $\Gamma = 0$ when there is no electromagnetic interference (the applied solutions eliminate the influence of electromagnetic interference on the track-side CCTV cabinet).
- $\Gamma = 1$ when solutions eliminating the influence of electromagnetic interferences on the track-side CCTV cabinet are not applied.

Therefore, having a specific solution, it is possible to estimate its impact on reducing the influence of electromagnetic interference on the functioning of the track-side CCTV cabinet. Thus, it is possible to quantify the factors of electromagnetic interference $\Gamma$.

A full ability $S_{PZ}$ is a state in which a track-side CCTV cabinet functions correctly. Impendency over safety I $S_{ZB1}$ is a state in which a track-side CCTV cabinet is partially fit (parallel coupling through a mutual impedance). Impendency over safety II $S_{ZB2}$ is a state in which a track-side CCTV cabinet is partially fit (parallel coupling through board capacity relative to the casing). The unreliability of safety $S_B$ is a state in which a track-side CCTV cabinet is unfit (electromagnetic interference exceeds limit values).

If a track-side CCTV cabinet is in a state of a full ability $S_{PZ}$ and the interference appears in the form of parallel coupling through a mutual impedance, then the system switches to a state of impendency over safety I $S_{ZB1}$ with the intensity of $\lambda_{ZB1}$. If the system is in the state of impendency over safety I $S_{ZB1}$, then it is possible to switch to the state of a full ability $S_{PZ}$ provided that actions are taken aimed at restoring the fitness state.

In the event of a state of impendency over safety I $S_{ZB1}$ and the interference exceeding permissible values, the system moves to a state of the unreliability of safety $S_B$ with an intensity of $\lambda_{B1}$.

If a track-side CCTV cabinet is in a state of full ability $S_{PZ}$ and the interference appears in the form of parallel coupling through board capacitance relative to the casing, then the system switches to a state of impendency over safety II $S_{ZB2}$ with the intensity of $\lambda_{ZB2}$. If the system is in the state of impendency over safety II $S_{ZB2}$, then it is possible to switch to the state of a full ability $S_{PZ}$, provided that actions aimed at restoring the fitness state are taken.

In the event of a state of impendency over safety II $S_{ZB2}$ and the interference exceeding permissible values, the system moves to a state of the unreliability of safety $S_B$ with an intensity of $\lambda_{B2}$.

If a track-side CCTV cabinet is in a state of impendency over safety II $S_{ZB2}$ and the interference changes from parallel coupling through a mutual impedance to interference in the form of parallel coupling through board capacitance relative to the casing, the system switches to a state of impendency over safety I $S_{ZB1}$ with the intensity of $\mu_{B0}$.

If a track-side CCTV cabinet is in a state of the unreliability of safety $S_B$ and actions are taken at restoring the state of fitness, then it switches to a state of full ability $S_{PZ}$ with the intensity of $\mu_{B1}$.

The exponential distribution to determine the individual safety states of the CCTV system operation process can be used considering preliminary aging, which is carried out in individual companies producing electronic components. The producer of a given element – in this case, the CCTV system cameras, determines the initial aging time, e.g. 2-4 days when the device is connected to the power supply and produces reference signals. After this time, the given device of the security system is subject to a technical inspection and is transferred to the recipient. Given the aging time, it can be assumed that the failure intensity $\lambda(t)$ of the individual elements constituting the safety system has a constant value. During the initial aging, the most damage occurs, this is known as the so-called age of the infant element.

The system shown in Fig. 9 can be described by the following Chapman–Kolmogorov equations:

$$
\begin{aligned}
R_0'(t) = &-\Gamma_{ZB1} \cdot \lambda_{ZB1} \cdot R_0(t) + \mu_{PZ1} \cdot Q_{ZB1}(t) \\
&- \Gamma_{ZB2} \cdot \lambda_{ZB2} \cdot R_0(t) + \mu_{PZ2} \cdot Q_{ZB2}(t) + \mu_B \cdot Q_B(t), \\
Q_{ZB1}'(t) = &\,\Gamma_{ZB1} \cdot \lambda_{ZB1} \cdot R_0(t) - \mu_{PZ1} \cdot Q_{ZB1}(t) \\
&- \Gamma_{B1} \cdot \lambda_{B1} \cdot Q_{ZB1}(t) + \Gamma_{B0} \cdot \mu_{B0} \cdot Q_{ZB2}(t), \\
Q_{ZB2}'(t) = &\,\Gamma_{ZB2} \cdot \lambda_{ZB2} \cdot R_0(t) - \mu_{PZ2} \cdot Q_{ZB2}(t) \\
&- \Gamma_{B2} \cdot \lambda_{B2} \cdot Q_{ZB2}(t) - \Gamma_{B0} \cdot \mu_{B0} \cdot Q_{ZB2}(t), \\
Q_B'(t) = &\,\Gamma_{B1} \cdot \lambda_{B1} \cdot Q_{ZB1}(t) + \Gamma_{B2} \cdot \lambda_{B2} \cdot Q_{ZB2}(t) \\
&- \mu_B \cdot Q_B(t).
\end{aligned}
\tag{2}
$$

Assuming the baseline conditions:

$$
\begin{aligned}
R_0(0) &= 1, \\
Q_{ZB1}(0) &= Q_{ZB2}(0) = Q_B(0) = 0,
\end{aligned}
\tag{3}
$$

and applying the Laplace transform, the following system of linear equations is obtained:

$$
\begin{aligned}
s \cdot R_0^*(s) - 1 = &-\Gamma_{ZB1} \cdot \lambda_{ZB1} \cdot R_0^*(s) + \mu_{PZ1} \cdot Q_{ZB1}^*(s) \\
&- \Gamma_{ZB2} \cdot \lambda_{ZB2} \cdot R_0^*(s) + \mu_{PZ2} \cdot Q_{ZB2}^*(s) \\
&+ \mu_B \cdot Q_B^*(s), \\
s \cdot Q_{ZB1}^*(s) = &\,\Gamma_{ZB1} \cdot \lambda_{ZB1} \cdot R_0^*(s) - \mu_{PZ1} \cdot Q_{ZB1}^*(s) \\
&- \Gamma_{B1} \cdot \lambda_{B1} \cdot Q_{ZB1}^*(s) + \Gamma_{B0} \cdot \mu_{B0} \cdot Q_{ZB2}^*(s), \\
s \cdot Q_{ZB2}^*(s) = &\,\Gamma_{ZB2} \cdot \lambda_{ZB2} \cdot R_0^*(s) - \mu_{PZ2} \cdot Q_{ZB2}^*(s) \\
&- \Gamma_{B2} \cdot \lambda_{B2} \cdot Q_{ZB2}^*(s) - \Gamma_{B0} \cdot \mu_{B0} \cdot Q_{ZB2}^*(s), \\
s \cdot Q_B^*(s) = &\,\Gamma_{B1} \cdot \lambda_{B1} \cdot Q_{ZB1}^*(s) + \Gamma_{B2} \cdot \lambda_{B2} \cdot Q_{ZB2}^*(s) \\
&- \mu_B \cdot Q_B^*(s).
\end{aligned}
\tag{4}
$$

Bull. Pol. Acad. Sci. Tech. Sci. 69(2) 2021, e136747

7

J. Paś, A. Rosiński, and K. Białek

Transforming it, a record in the schematic view is obtained:

$$R_0^*(s) = -\Big(b_1 \cdot b_2 \cdot c\Big)\Big/\Big(b_2 \cdot c \cdot \Gamma_{ZB1} \cdot \lambda_{ZB1} \cdot \mu_{PZ1}$$
$$- a \cdot b_1 \cdot b_2 \cdot c + b_1 \cdot c \cdot \Gamma_{ZB2} \cdot \lambda_{ZB2} \cdot \mu_{PZ2}$$
$$+ b_2 \cdot \Gamma_{B1} \cdot \lambda_{B1} \cdot \mu_B \cdot \Gamma_{ZB1} \cdot \lambda_{ZB1} + b_1 \cdot \Gamma_{B2}$$
$$\cdot \lambda_{B2} \cdot \mu_B \cdot \Gamma_{ZB2} \cdot \lambda_{ZB2} + c \cdot \Gamma_{B0} \cdot \mu_{B0} \cdot \mu_{PZ1}$$
$$\cdot \Gamma_{ZB2} \cdot \lambda_{ZB2} + \Gamma_{B1} \cdot \lambda_{B1} \cdot \Gamma_{B0} \cdot \mu_{B0} \cdot \mu_B \cdot \Gamma_{ZB2} \cdot \lambda_{ZB2}\Big),$$

$$Q_{ZB1}^*(s) = -\Big(b_2 \cdot c \cdot \Gamma_{ZB1} \cdot \lambda_{ZB1} + c \cdot \Gamma_{B0} \cdot \mu_{B0} \cdot \Gamma_{ZB2} \cdot \lambda_{ZB2}\Big)\Big/$$
$$\Big(b_2 \cdot c \cdot \Gamma_{ZB1} \cdot \lambda_{ZB1} \cdot \mu_{PZ1} - a \cdot b_1 \cdot b_2 \cdot c$$
$$+ b_1 \cdot c \cdot \Gamma_{ZB2} \cdot \lambda_{ZB2} \cdot \mu_{PZ2} + b_2 \cdot \Gamma_{B1} \cdot \lambda_{B1}$$
$$\cdot \mu_B \cdot \Gamma_{ZB1} \cdot \lambda_{ZB1} + b_1 \cdot \Gamma_{B2} \cdot \lambda_{B2} \cdot \mu_B$$
$$\cdot \Gamma_{ZB2} \cdot \lambda_{ZB2} + c \cdot \Gamma_{B0} \cdot \mu_{B0} \cdot \mu_{PZ1} \cdot \Gamma_{ZB2} \cdot \lambda_{ZB2}$$
$$+ \Gamma_{B1} \cdot \lambda_{B1} \cdot \Gamma_{B0} \cdot \mu_{B0} \cdot \mu_B \cdot \Gamma_{ZB2} \cdot \lambda_{ZB2}\Big),$$

$$Q_{ZB2}^*(s) = -\Big(b_1 \cdot c \cdot \Gamma_{ZB2} \cdot \lambda_{ZB2}\Big)\Big/\Big(b_2 \cdot c \cdot \Gamma_{ZB1} \cdot \lambda_{ZB1} \cdot \mu_{PZ1}$$
$$- a \cdot b_1 \cdot b_2 \cdot c + b_1 \cdot c \cdot \Gamma_{ZB2} \cdot \lambda_{ZB2} \cdot \mu_{PZ2} \qquad (5)$$
$$+ b_2 \cdot \Gamma_{B1} \cdot \lambda_{B1} \cdot \mu_B \cdot \Gamma_{ZB1} \cdot \lambda_{ZB1} + b_1 \cdot \Gamma_{B2} \cdot \lambda_{B2}$$
$$\cdot \mu_B \cdot \Gamma_{ZB2} \cdot \lambda_{ZB2} + c \cdot \Gamma_{B0} \cdot \mu_{B0} \cdot \mu_{PZ1} \cdot \Gamma_{ZB2} \cdot \lambda_{ZB2}$$
$$+ \Gamma_{B1} \cdot \lambda_{B1} \cdot \Gamma_{B0} \cdot \mu_{B0} \cdot \mu_B \cdot \Gamma_{ZB2} \cdot \lambda_{ZB2}\Big),$$

$$Q_B^*(s) = -\Big(b_2 \cdot \Gamma_{B1} \cdot \lambda_{B1} \cdot \Gamma_{ZB1} \cdot \lambda_{ZB1} + b_1 \cdot \Gamma_{B2} \cdot \lambda_{B2}$$
$$\cdot \Gamma_{ZB2} \cdot \lambda_{ZB2} + \Gamma_{B1} \cdot \lambda_{B1} \cdot \Gamma_{B0} \cdot \mu_{B0} \cdot \Gamma_{ZB2} \cdot \lambda_{ZB2}\Big)\Big/$$
$$\Big(b_2 \cdot c \cdot \Gamma_{ZB1} \cdot \lambda_{ZB1} \cdot \mu_{PZ1} - a \cdot b_1 \cdot b_2 \cdot c + b_1 \cdot c \cdot \Gamma_{ZB2}$$
$$\cdot \lambda_{ZB2} \cdot \mu_{PZ2} + + b_2 \cdot \Gamma_{B1} \cdot \lambda_{B1} \cdot \mu_B \cdot \Gamma_{ZB1} \cdot \lambda_{ZB1}$$
$$+ b_1 \cdot \Gamma_{B2} \cdot \lambda_{B2} \cdot \mu_B \cdot \Gamma_{ZB2} \cdot \lambda_{ZB2} + c \cdot \Gamma_{B0} \cdot \mu_{B0} \cdot \mu_{PZ1}$$
$$\cdot \Gamma_{ZB2} \cdot \lambda_{ZB2} + \Gamma_{B1} \cdot \lambda_{B1} \cdot \Gamma_{B0} \cdot \mu_{B0} \cdot \mu_B \cdot \Gamma_{ZB2} \cdot \lambda_{ZB2}\Big),$$

where:

$$a = s + \Gamma_{ZB1} \cdot \lambda_{ZB1} + \Gamma_{ZB2} \cdot \lambda_{ZB2},$$
$$b_1 = s + \mu_{PZ1} + \Gamma_{B1} \cdot \lambda_{B1},$$
$$b_2 = s + \mu_{PZ2} + \Gamma_{B2} \cdot \lambda_{B2} + \Gamma_{B0} \cdot \mu_{B0},$$
$$c = s + \mu_B.$$

By conducting further mathematical analysis, we obtain relationships, which allow the determination of probabilities of a system staying in states of full ability S$_{PZ}$, impendency over safety S$_{ZB1}$ and S$_{ZB2}$, and the unreliability of safety $_B$.

## 3. Modelling the operation process of a track-side CCTV cabinet, considering electromagnetic interference

Simulations and computer research provide an opportunity to determine the influence of reliability and operational parameters of individual elements on the entire system [57].

With the use of computer assistance, it is possible to conduct calculations enabling the determination of the probability value for a track-side CCTV cabinet to be in a state of full ability S$_{PZ}$. Such a procedure is shown in the following example.

**Example**

Let us assume the following values describing the analysed system:

- The duration of research – 1 year (the value of this time is given in the units as hours [h]):
$$t = 8760 \text{ [h]};$$
- The intensity of transitions from a state of full ability to a state of impendency over safety I $\lambda_{ZB1}$:
$$\lambda_{ZB1} = 0.000001;$$
- The intensity of transitions from a state of full ability to a state of impendency over safety II $\lambda_{ZB2}$:
$$\lambda_{ZB2} = 0.0000001;$$
- The intensity of transitions from a state of impendency over safety I to a state of the unreliability of safety $\lambda_{B1}$:
$$\lambda_{B1} = 0.0000001;$$
- The intensity of transitions from a state of impendency over safety II to a state of the unreliability of safety $\lambda_{N2}$:
$$\lambda_{B2} = 0.000001;$$
- The intensity of transitions from a state of impendency over safety II to a state of impendency over safety I $\mu_{B0}$:
$$\mu_{B0} = 0.00000001;$$
- The intensity of transitions from a state of the unreliability of safety to a state of full ability $\mu_{B1}$:
$$\mu_B = 0.01;$$
- The intensity of transitions from a state of impendency over safety I to a state of full ability $\mu_{PZ1}$:
$$\mu_{PZ1} = 0.1;$$
- The intensity of transitions from a state of impendency over safety II to a state of full ability $\mu_{PZ2}$:
$$\mu_{PZ2} = 0.2.$$

The following is obtained for the above input values, using Eq. (5):

$$R_0^*(s) = \Big(1.1100101 \cdot 10^{14} \cdot s + 1.01 \cdot 10^{14} \cdot \mu_{PZ1}$$
$$+ 1 \cdot 10^{13} \cdot \mu_{PZ2} + 1 \cdot 10^{22} \cdot s^2 \cdot \mu_{PZ1} + 1 \cdot 10^{22} \cdot s^2 \cdot \mu_{PZ2}$$
$$+ 1.000111 \cdot 10^{20} \cdot s^2 + 1 \cdot 10^{22} \cdot s^3 + 1.000101 \cdot 10^{20} \cdot s \cdot \mu_{PZ1}$$
$$+ 1.00001 \cdot 10^{20} \cdot s \cdot \mu_{PZ2} + 1 \cdot 10^{20} \cdot \mu_{PZ1} \cdot \mu_{PZ2}$$
$$+ 1 \cdot 10^{22} \cdot s \cdot \mu_{PZ1} \cdot \mu_{PZ2} + 1.01 \cdot 10^7\Big)$$
$$\Big/\Big(1.12201111 \cdot 10^8 \cdot s + 1.000111 \cdot 10^{20} \cdot s^2 \cdot \mu_{PZ1}$$
$$+ 1.00011 \cdot 10^{20} \cdot s^2 \cdot \mu_{PZ2} + 1 \cdot 10^{22} \cdot s^3 \cdot \mu_{PZ1}$$
$$+ 1 \cdot 10^{22} \cdot s^3 \cdot \mu_{PZ2} + 2.2101322 \cdot 10^{14} \cdot s^2$$
$$+ 1.000221 \cdot 10^{20} \cdot s^3 + 1 \cdot 10^{22} \cdot s^4$$
$$+ 1.11001 \cdot 10^{14} \cdot s \cdot \mu_{PZ1} + 1.10001 \cdot 10^{14} \cdot s \cdot \mu_{PZ2}$$
$$+ 1 \cdot 10^{20} \cdot s \cdot \mu_{PZ1} \cdot \mu_{PZ2} + 1 \cdot 10^{22} \cdot s^2 \cdot \mu_{PZ1} \cdot \mu_{PZ2}\Big).$$

8

Bull. Pol. Acad. Sci. Tech. Sci. 69(2) 2021, e136747

As a result of transformations, we obtain:

$$R_0(t) = 1.63738476 \cdot 10^{-10} \cdot e^{-0.01 \cdot t}$$
$$+ 5.0000454339 \cdot 10^{-7} \cdot e^{-0.20000111 \cdot t}$$
$$+ 0.00000999985 \cdot e^{-0.10000109 \cdot t} + 0.99998949997.$$

As a final result, we obtain: $R_O = 0.99998949$.

The presented reliability-operational analysis of a track-side CCTV cabinet, considering the electromagnetic interference, enables numerical evaluation of different types of solutions (technical and organizational). As a result, they can be implemented, in order to minimize the impact of electromagnetic interference on the functioning of a track-side CCTV cabinet.

To sum up the considerations, it can be concluded that if the designers of track-side CCTV cabinets operated in rail transport are aware of the conditions of an electromagnetic environment, i.e. through the measurements and reliability-operational analysis presented above) in which a system is to be probably functioning, then it is necessary to meet the EMC requirements, which are usually known and can be considered at the device engineering stage.

## 4. Conclusions

Using electronic systems in track-side CCTV cabinets means they need to function in various electromagnetic environment conditions, within a vast railway area, often with very close proximity to each other. The consequence may be an increased level of electromagnetic interference, which impacts other systems located in this part of a railway area (external compatibility). This can cause incorrect functioning of both a track-side CCTV cabinet and rail traffic control systems; hence, the presence of these devices in the states of impendency over safety or the unreliability of safety. Therefore, when designing CCTV cabinets, it is important to plan their operation in actual conditions, namely, among other electronic and electric devices (a given electromagnetic environment). The presented reliability-operational analysis of a track-side CCTV cabinet, considering electromagnetic interference, may become helpful in that matter. It facilitates the numerical determination of the probabilities of a track-side CCTV cabinet staying in the distinguished states.

In further research concerning this issue (electromagnetic field impact), the authors plan the development of further reliability-operational models, which will involve varied states of impendency over safety. This will allow more accurate mapping of track-side CCTV cabinet functioning in an electromagnetic railway environment and other critical infrastructure facilities.

## REFERENCES

[1] R. Gordon, *Intelligent Freeway Transportation Systems: Functional Design*, Springer Science+Business Media, 2009.

[2] P. Łubkowski and D. Laskowski, "Selected Issues of Reliable Identification of Object in Transport Systems Using Video Monitoring Services", in *Communication in Computer and Information Science*, vol. 471, pp. 59–68, Springer, Berlin Heidelberg, 2015.

[3] M. Siergiejczyk, A. Rosiński, and J. Paś, "Analysis of unintended electromagnetic fields generated by safety system control panels", *Diagnostyka* 17(3), 35–40 (2016).

[4] M. Siergiejczyk, J. Paś, and A. Rosiński, "Train call recorder and electromagnetic interference". *Diagnostyka* 16(1), 19–22 (2015).

[5] K. Sunitha and M. Joy Thomas, "Effect of Soil Conditions on the Electromagnetic Field From an Impulse Radiating Antenna and on the Induced Voltage in a Buried Cable", *IEEE Trans. Electromagn. Compat.* 61(4), 990–997 (2019), doi: 10.1109/TEMC.2018.2844205.

[6] M. Kornaszewski, M. Chrzan, and Z. Olczykowski, "Implementation of New Solutions of Intelligent Transport Systems in Railway Transport in Poland", in *Communications in Computer and Information Science*, pp. 282–292, Springer, 2017.

[7] J. Dyduch, J. Paś, and A. Rosiński, *The basic of the exploitation of transport electronic systems*, Publishing House of Radom University of Technology, Radom, 2011.

[8] J. Paś, *Operation of electronic transportation systems*, Publishing House University of Technology and Humanities, Radom, 2015.

[9] M. Chrzan, M. Kornaszewski, and T. Ciszewski, "Renovation of Marine Telematics Objects in the Process of Exploitation", in *Communications in Computer and Information Science*, pp. 337–351, Springer, 2018.

[10] M. Siergiejczyk, J. Paś, and E. Dudek, "Reliability analysis of aerodrome's electronic security systems taking into account electromagnetic interferences", in *Risk, Reliability and Safety: Innovating Theory and Practice: Proceedings of ESREL 2016*, pp. 2285–2292, eds. L. Walls, M. Revie, and T. Bedford, CRC Press/Balkema, 2017.

[11] A. Rosiński, *Modelling the maintenance process of transport telematics systems*, Publishing House Warsaw University of Technology, Warsaw, 2015.

[12] D. Romero-Faz and A. Camarero-Orive, "Risk assessment of critical infrastructures – New parameters for commercial ports", *Int. J. Crit. Infor. Prot.* 18, 50–57 (2017).

[13] M. Jacyna, J. Żak, and P. Gołębiowski, "The EMITRANSYS model and the possibilities of its application for the analysis of the development of sustainable transport systems", *Combust. Eng.* 179(4), 243–248 (2019).

[14] R. Billinton and R.N. Allan, *Reliability evaluation of power systems*, Plenum Press, New York, 1996.

[15] R. Hari Kumar, N. Mayadevi, V.P. Mini, and S. Ushakumari, "Transforming distribution system into a sustainable isolated microgrid considering contingency", *Bull. Pol. Acad. Sci. Tech. Sci.* 67(5), 871–881 (2019).

[16] R. Matyszkiel, R. Polak, P. Kaniewski, and D. Laskowski, "The results of transmission tests of polish broadband SDR radios", in *Communication and Information Technologies (KIT)*, pp. 1–6, Slovakia, 2017.

[17] A. Kierzkowski and T. Kisiel, "Simulation model of security control system functioning: A case study of the Wroclaw Airport terminal", *J. Air. Transp. Manag.* 64(B), 173–185 (2016).

[18] D. Caban and T. Walkowiak, "Dependability analysis of hierarchically composed system-of-systems", in *Proceedings of the Thirteenth International Conference on Dependability and Complex Systems DepCoS-RELCOMEX*, pp. 113–120, eds. W. Zamojski, J. Mazurkiewicz, J. Sugier, T. Walkowiak, and J. Kacprzyk, Springer, 2019.

Bull. Pol. Acad. Sci. Tech. Sci. 69(2) 2021, e136747

9

[19] M. Borecki, M. Ciuba, Y. Kharchenko, and Y. Khanas, "Substation reliability evaluation in the context of the stability prediction of power grids", *Bull. Pol. Acad. Sci. Tech. Sci.* 68(4), 769–776 (2020).

[20] M. Siergiejczyk, K. Krzykowska, and A. Rosiński, "Evaluation of the influence of atmospheric conditions on the quality of satellite signal", in *Marine Navigation*, pp. 121–128, ed. A. Weintrit, CRC Press/Balkema, London, 2017.

[21] M. Stawowy and P. Dziula, "Comparison of uncertainty multilayer models of impact of teleinformation devices reliability on information quality", in *Proceedings of the European Safety and Reliability Conference ESREL 2015*, pp. 2685–2691, eds. L. Podofillini, B. Sudret, B. Stojadinovic, E. Zio, and W. Kröger, CRC, Press/Balkema, 2015.

[22] M. Stawowy and Z. Kasprzyk, "Identifying and simulation of status of an ICT system using rough sets", in *Proceedings of the Tenth International Conference on Dependability and Complex Systems DepCoS-RELCOMEX*, pp. 477–484, eds. Z. Zamojski, J. Mazurkiewicz, J. Sugier, T. Walkowiak, and J. Kacprzyk, Springer, 2015.

[23] T. Dabrowski, M. Bednarek, K. Fokow, and M. Wisnios, "The method of threshold-comparative diagnosing insensitive on disturbances of diagnostic signals", *Prz. Elektrotechniczny – Electrical Review* 88(11A), 93–97 (2012).

[24] M. Łabowski and P. Kaniewski, "Motion Compensation for Unmanned Aerial Vehicle's Synthetic Apperture Radar", in *Signal Processing Symposium SPSympo 2015*, Debe, 2015, pp.184–188.

[25] P. Kaniewski, R. Gil, and S. Konatowski, "Estimation of UAV Position with Use of Smoothing Algorithms", *Metrol. Meas. Syst.* 24(1), 127–142 (2017).

[26] K. Reddig, B. Dikunow, and K. Krzykowska, "Proposal of big data route selection methods for autonomous vehicles", *Internet Technol. Lett.* 1(36), 1–6 (2018).

[27] S. Duer, R. Duer, and S. Mazuru, "Determination of the expert knowledge base on the basis of a functional and diagnostic analysis of a technical object", *Romanian Association of Nonconventional Technologies* XX(2), 23–29 (2016).

[28] S. Duer, K. Zajkowski, I. Płocha, and R. Duer, "Training of an artificial neural network in the diagnostic system of a technical object", *Neural Comput. Appl.* 22(7), 1581–1590 (2013).

[29] F. Losurdo, I. Dileo, M. Siergiejczyk, K. Krzykowska, and M. Krzykowski, "Innovation in the ICT infrastructure as a key factor in enhancing road safety. A multi-sectoral approach", in *Proceedings 25th International Conference on Systems Engineering ICSEng 2017*, pp. 157–162, eds. H. Selvaraj, G. Chmaj, and D. Zydek, 2017.

[30] R. Burdzik, Ł. Konieczny, and T. Figlus, "Concept of on-board comfort vibration monitoring system for vehicles", in *Activities of Transport Telematics*, pp. 418–425, ed. J. Mikulski, Springer, Heidelberg, 2013.

[31] M. Kostrzewski, "Analysis of selected acceleration signals measurements obtained during supervised service conditions – study of hitherto approach", *J. Vibroeng.* 20(4), 1850–1866 (2018).

[32] M. Ali Niknejad, *Electromagnetics for High-Speed Analog and Digital Communication Circuits*, Cambridge University Press, 2007.

[33] S. Piersanti, A. Orlandi, and F. de Paulis, "Electromagnetic Absorbing materials design by optimization using a machine learning approach", *IEEE Trans. Electromagn. Compat.* 1–8 (2018), doi: 10.1109/TEMC.2018.2871879.

[34] J. Vašata and R. Doleček, "Electromagnetic compatibility and lightning current impacts in the railway equipment buildings", in *26th Conference Radioelektronika 2016*, Košice, Slovak Republic, 2016.

[35] E. Lheurette, *Metamaterials and Wave Control*, ISTE and Wiley, 2013.

[36] H. Urbancokova, J. Valouch, and M. Adamek, "Testing of an Intrusion and Hold-up Systems for Electromagnetic Susceptibility – EFT/B", *Int. J. Circuits Syst. Signal Process.* 9, 40–46 (2015).

[37] J. Valouch, "Technical requirements for Electromagnetic Compatibility of Alarm Systems", *Int. J. Circuits Syst. Signal Process.* 9, 186–191 (2015).

[38] S. Kovaf, J. Valouch, H. Urbančoková, and M. Adámek, "Electromagnetic interference of CCTV", in *International Conference on Information and Digital Technologies*, Zilina, 2015, pp. 172–177.

[39] S. Kovář, J. Valouch, H. Urbančoková, and M. Adámek, "Impact of security cameras on electromagnetic environment in far and near-field", in *International Conference on Information and Digital Technologies (IDT) 2016*, Rzeszow, 2016, pp. 156–159.

[40] H. Urbancokova and J. Valouch, "Monitoring of the tests EMS information technology equipment using the CCTV system", *Int. J. Circuits Syst. Signal Process.* 9, 9–15 (2015).

[41] H. Urbancokova, S. Kovar, O. Halaska, and J. Valouch, "Immunity of electronic devices against radio-frequency electromagnetic fields", in *21st International Conference on Circuits, Systems, Communications and Computers (CSCC 2017)*, MATEC Web of Conferences, vol. 125, 2017.

[42] R.D. White, L.M. McCormack, and P.W. Hooper, "Electrical System Integration, Electromagnetic Compatibility (EMC) Interface Management of Railway Electrification Systems". *HKIE Trans.* 13 (1), 55–59 (2006).

[43] Z. Wróbel, "The Electromagnetic Compatibility in Researches of Railway Traffic Control Devices", in *Analysis and Simulation of Electrical and Computer Systems*, pp. 275–287, eds. D. Mazur, M. Gołębiowski, and M. Korkosz, Springer, 2018.

[44] M. Urbaniak, E. Kardas-Cinal, and M. Jacyna, "Optimization of energetic train cooperation", *Symmetry* 11(1175), (2019).

[45] E. Masson, M. Berbineau, *Broadband Wireless Communications for Railway Applications, Studies in Systems, Decision and Control*, Springer International Publishing, 2017.

[46] PN-EN 55016-4-2:2011 + A1:2014. Specification for radio disturbance and immunity measuring apparatus and methods – Part 4–2: Uncertainties, statistics and limit modelling – Measurement instrumentation uncertainty.

[47] PN-EN 55016-2-3:2017. Specification for radio disturbance and immunity measuring apparatus and methods – Part 2–3: Methods of measurement of disturbances and immunity – Radiated disturbance measurements.

[48] PN-EN 50121-3-2:2017. Railway applications – Electromagnetic compatibility – Part 3–2: Rolling stock – Apparatus.

[49] PN-EN 61000-6-4:2008 + A1:2012. Electromagnetic compatibility (EMC) – Part 6–4: Generic standards – Emission standard for industrial environments.

[50] R. Smolenski, P. Lezynski, J. Bojarski, W. Drozdz, and L.C. Long, "Electromagnetic compatibility assessment in multiconverter power systems – Conducted interference issues", *Measurement* 165, 1–8 (2020).

[51] V. Kuznetsov, B. Lyubarskyi, E. Kardas-Cinal, B. Yeritsyan, I. Riabov, and I. Rubanik, "Recommendations for the selection of parameters for shunting locomotives", *Arch. Transp.* 56(4), 119–133 (2020).

10

Bull. Pol. Acad. Sci. Tech. Sci. 69(2) 2021, e136747

[52] C. Alcaraz and S. Zeadally, "Critical infrastructure protection: Requirements and challenges for the 21st century", *Int. J. Crit. Infrastruct. Prot.* 8, 53–66 (2015).

[53] M. Stawowy and M. Siergiejczyk, "Application and simulations of uncertainty multilevel models to ensure the ITS services", in *Risk, Reliability and Safety: Innovating Theory and Practice: Proceedings of ESREL 2016*, pp. 601–605, eds. L. Walls, M. Revie, and T. Bedford, CRC Press/Balkema, 2017.

[54] D. Szmel, W. Zabłocki, P. Ilczuk, and A. Kochan, "Selected issues of risk assessment in relation to railway signalling systems", *WUT J. Transp. Eng.* 127, 81–91 (2019).

[55] J. Paś and T. Klimczak, "Selected issues of the reliability and operational assessment of a fire alarm system", *Eksploatacja i Niezawodnosc–Maintenance and Reliability* 21(4), 553–561 (2019).

[56] M. Siergiejczyk, A. Rosiński, P. Dziula, and K. Krzykowska, "Reliability-exploitation analysis of highway transport telematics systems", *J. KONBiN* 1(33), 177–186 (2015).

[57] J. Paś, A. Rosiński, M. Chrzan, and K. Białek, "Reliability-Operational Analysis of the LED Lighting Module Including Electromagnetic Interference", *IEEE Trans. Electromagn. Compat.* 62(6), 2747–2758 (2020).

Bull. Pol. Acad. Sci. Tech. Sci. 69(2) 2021, e136747

11